

Energy-Aware Competitive Power Allocation for Heterogeneous Networks Under QoS Constraints

Giacomo Bacci, *Member, IEEE*, E. Veronica Belmega, *Member, IEEE*,
 Panayotis Mertikopoulos, *Member, IEEE* and Luca Sanguinetti, *Member, IEEE*

Abstract

This work proposes a distributed power allocation scheme for maximizing energy efficiency in the uplink of orthogonal frequency-division multiple access (OFDMA)-based heterogeneous networks (HetNets). The user equipment (UE) in the network are modeled as rational agents that engage in a non-cooperative game where each UE allocates its available transmit power over the set of assigned subcarriers so as to maximize its individual utility (defined as the user's throughput per Watt of transmit power) subject to minimum-rate constraints. In this framework, the relevant solution concept is that of Debreu equilibrium, a generalization of Nash equilibrium which accounts for the case where an agent's set of possible actions depends on the actions of its opponents. Since the problem at hand might not be feasible, Debreu equilibria do not always exist. However, using techniques from fractional programming, we provide a characterization of equilibrial power allocation profiles when they do exist. In particular, Debreu equilibria are found to be the fixed points of a water-filling best response operator whose water level is a function of minimum rate constraints and circuit power. Moreover, we also describe a set of sufficient conditions for the existence and uniqueness of Debreu equilibria exploiting the contraction properties of the best response operator. This analysis provides the necessary tools to derive a power allocation scheme that steers the network to equilibrium in an iterative and distributed manner without the need for any centralized processing. Numerical simulations are then used to validate the analysis and assess the performance of the proposed algorithm as a function of the system parameters, also discussing key design tradeoffs to meet 5G requirements (e.g., obtaining more than 500 b/s/Hz/km² area spectral efficiency) with a reasonable amount of physical resources (e.g., bandwidth and transmit power), and of complexity at the receiving stations, such as minimal information requirements at the user level and number of antennas.

Index Terms

G. Bacci and L. Sanguinetti are with the Department of Information Engineering, University of Pisa, 56126 Pisa, Italy (email: giacomo.bacci@iet.unipi.it, luca.sanguinetti@iet.unipi.it). G. Bacci is also with the Department of Electrical Engineering, Princeton University, Princeton, NJ 08544 USA. L. Sanguinetti is also with Alcatel-Lucent Chair, Ecole Supérieure d'Électricité (Supélec), 91190 Gif-sur-Yvette, France.

E. V. Belmega is with ETIS/ENSEA, Université de Cergy-Pontoise, 95014 Cergy-Pontoise, France (email: elena-veronica.belmega@ensea.fr).

P. Mertikopoulos is with the French National Center for Scientific Research (CNRS) and the Laboratoire d'Informatique de Grenoble, Grenoble, France (email: panayotis.mertikopoulos@imag.fr).

Heterogeneous networks; 5G communications; energy efficiency; area spectral efficiency; power allocation policy; distributed algorithms; game theory; Debreu equilibrium; QoS requirements.

I. INTRODUCTION

Owing to the prolific spread of Internet-enabled mobile devices and the ever-growing volume of mobile communications, the biggest challenge in the wireless industry today is to meet the soaring demand for wireless broadband required to ensure consistent quality of service (QoS) in a network. Rising to this challenge means increasing the network capacity by a thousandfold over the next few years [1], but the resulting power consumption and energy-related pollution are expected to give rise to major societal, economic, and environmental issues that would render this growth unsustainable [2, 3]. In this way, the information and communications technology (ICT) industry is faced with a formidable mission: cellular network capacity must be increased significantly in order to accommodate higher data rates, but this task must be accomplished under an extremely tight energy budget.

A promising way out of this gridlock is the small-cell (SC) network paradigm which builds on the premise of shrinking wireless cell sizes in order to bring user equipment (UE) and their serving stations closer to one another. More precisely, an SC network is composed of a mix of operator-installed low-cost/low-power base stations (with broadly varying capabilities and technical specifications), all endowed with multiple antennas and equipped with advanced self-organization functionalities. Thus, from an operational standpoint, SC networks can be integrated seamlessly into existing macro-cellular networks: the latter ensure wide-area coverage and support for mobility, while the former carry most of the generated data traffic [4].

Albeit promising, the deployment of this kind of networks, commonly referred to as heterogeneous networks (HetNets), poses several key technical challenges, mainly because different small cells are likely to be connected over unreliable backhaul infrastructures with widely varying features and characteristics – such as error rate, outage, delay, and/or capacity specifications. Accordingly, the inherently heterogeneous nature of these networks calls for flexible and decentralized resource allocation strategies that rely only on local channel state information (CSI) and require minimal information exchange between network users and/or access points/base stations. This framework is commonly referred to as *distributed optimization* and it represents a crucial aspect of scalable and efficient network operation.

An established theoretical toolbox for problems of this kind is provided by the theory of noncooperative games [5]. Among the early contributions in this area, [6–8] investigated the rate maxi-

mization problem for autonomous digital subscriber lines based on competitive optimality criteria. Following the spirit of these works, a vast corpus of literature has since focused on developing power control techniques for unilateral spectral efficiency maximization subject to individual power constraints. For instance, [9–11] proposed a game-theoretic approach to energy-efficient power control in multi-carrier code division multiple access (CDMA) systems, [12–16] investigated the problem of distributed power control in multi-user multiple-input and multiple-output (MIMO) systems, [17, 18] studied the interference relay channel, and two-tier CDMA networks were examined in [19]. More recently, the authors of [20] used a variational inequality (VI) framework to model and analyze the competitive spectral efficiency maximization problem. The resulting analogy between Nash equilibria and VIs is then exploited in [21] to design distributed power control algorithms for spectral efficiency maximization under interference temperature constraints in a cognitive radio context.

Distributed power allocation policies as above have the great advantage of avoiding the waste of energy associated with centralized algorithms that require considerable information exchange (and, hence, transmissions) between the users and/or the network administrator [20]. On the other hand, the users’ aggressive attitude towards interference from other users can lead to a cascade of power increases at the UE level, thereby leading to battery depletion and inefficient energy use. Consequently, solutions that focus exclusively on spectral efficiency maximization are not aligned with energy-efficiency requirements [22, 23] – which, as we mentioned above, are crucial for the deployment and operation of HetNets.

Summary of contributions: Our main goal in this paper is the analysis and design of energy-efficient power allocation policies in a HetNet setting where small-cell networks coexist with macro-tier cellular systems based on orthogonal frequency-division multiple access (OFDMA) technology. In particular, focusing on the uplink case, we propose a game-theoretic framework where each UE adjusts the allocation of its transmit power (over the available subcarriers) so as to maximize unilaterally its individual link utility subject to a minimum rate requirement that must be satisfied. Specifically, each user’s energy-aware utility function is defined as the achieved throughput per unit power, accounting for both the power required for data transmission and that required by the circuit components of each UE (such as amplifiers, mixer, oscillator, and filters) [24–26].

Due to each user’s rate constraints, the resulting game departs from the classical framework put forth by Nash [27] and gives rise to a Debreu-type game [28] where the actions available to each UE depend on the transmit power profile of all other users in the network. In this setting, the relevant solution concept is that of a *Debreu equilibrium* (DE) [28] – also known as a generalized

Nash equilibrium (GNE) [29]. Drawing on fractional programming techniques [30], we characterize the system's Debreu equilibria as fixed points of a water-filling operator whose water level is a function of the users' minimum rate constraints and circuit power [26]. This characterization is then used to provide sufficient conditions for DE uniqueness and to derive a distributed power allocation algorithm that allows the network to converge to equilibrium under minimal information assumptions. The performance of the proposed solution is then validated by means of extensive numerical simulations modeling a HetNet where a macro-tier is augmented with a certain number of low range small-cell access points (SCAs). As it turns out, the proposed solution represents a scalable and flexible technique to meet the ambitious goals of next-generation, 5G communications, such as extremely high area spectral efficiency (ASE) (more than 500 b/s/Hz/km²) with a reasonable amount of physical resources (bandwidth and power) and complexity at the network (number of small cells, signal processing burden, and number of transmit and receive antennas).

Related works: Our work builds on the game-theoretic analysis proposed in [31] where a group of players aims at maximizing their individual energy efficiency (EE) (decodable bits per Watts of transmit power) subject to each user's power constraints. Despite this similarity, the analysis of [31] does not account for minimum rate requirements, so the resulting game-theoretic model is a standard Nash game with no QoS guarantees – in particular, the users' rates at equilibrium could be fairly low. Incorporating QoS requirements changes the setting drastically and takes us beyond the standard Nash framework because a user's admissible power allocation policies depend crucially on the transmit powers of all other users. Preliminary versions of our results appeared in the conference papers [32, 33]: in contrast to these earlier papers, we provide here a complete equilibrium analysis and characterization along with sufficient conditions that guarantee the convergence of the system to a stable equilibrium state. Moreover, we also provide a detailed set of simulations specifically tailored for the HetNet scenario under study.

Paper outline: The remainder of this paper is organized as follows. In Section II, we introduce the system model and the EE maximization problem with minimum rate constraints. In Section III, we first formulate the noncooperative game and then study the existence and uniqueness of the Debreu equilibrium. Section IV presents an iterative and distributed algorithm to reach the equilibrium point, whereas Section V reports numerical results that are used to assess the performance of the proposed solution and to make comparisons with alternatives. Conclusions and perspectives are presented in Section VI while the proofs of our theoretical results are collected in a series of appendices at the end of the paper.

Notation: Matrices and vectors are denoted by bold letters, \mathbf{I}_L , $\mathbf{0}_L$, and $\mathbf{1}_L$ are the $L \times L$ identity matrix, the $L \times 1$ all-zero column vector, and the $L \times 1$ all-one column vector, respectively, and $\|\cdot\|$, $(\cdot)^T$ and $(\cdot)^H$ denote Euclidean norm of the enclosed vector, transposition and Hermitian transposition respectively. The notation $(x)^+$ stands for $\max\{0, x\}$ whereas $W(\cdot)$ denotes the Lambert W function [34], defined to be the multivalued inverse of the function $z = W(z) e^{W(z)}$ for any $z \in \mathbb{C}$. $\mathbb{1}_X$ denotes the indicator function such that $\mathbb{1}_X = 1$ if X is true, and 0 elsewhere. Finally, if \mathcal{A}_k , $k = 1, \dots, K$ is a finite family of sets, and $a_k \in \mathcal{A}_k$, we will use the notation $(a_k; \mathbf{a}_{-k}) \in \prod_k \mathcal{A}_k$ as shorthand for the profile $(a_1, \dots, a_k, \dots, a_K)$.

II. SYSTEM MODEL AND PROBLEM FORMULATION

A. System model

We consider the uplink of a HetNet where S low-range SCAs are adjoined to a macro-tier cell operating in an OFDMA-based open-access licensed spectrum. For compactness of notation, let us denote the macrocell base station (MBS) by index $s = 0$, so that $\mathcal{S} = \{0, 1, \dots, S\}$ represents the set of HetNet receiving stations. The s -th cell uses a set of orthogonal subcarriers to serve the K_s user equipment (UE) falling within its coverage radius ρ_s . For simplicity, we assume that the same set of subcarriers $\mathcal{N} = \{1, \dots, N\}$ is used by both tiers. We also assume that \mathcal{N} is assigned by the network and cannot be controlled by the cell operators. Each cell access point (AP) is further equipped with M_s receiving antennas, whereas a single antenna is employed at the UE to keep the complexity of the front-end limited. The framework described in the paper can be generalized to the case of a multicellular HetNet scenario, including MIMO configurations, in a straightforward manner.

Let $\mathbf{h}_{kj,n} \in \mathbb{C}^{M_{\psi(k)} \times 1}$ denote the uplink channel vector with entries $[\mathbf{h}_{kj,n}]_m$ representing the (frequency) channel gains over subcarrier n from the j -th UE to the m -th receive antenna of the serving AP $\psi(k)$ of user k , where $\psi(k) : \mathcal{K} \mapsto \mathcal{S}$ is a generic function that assigns each user k its serving AP.¹ In the following, $\mathcal{K} = \{1, \dots, K\}$ and $K = \sum_{s=0}^S K_s$ denote the set and the number of UE in the network, respectively, where K_s represents the number of UE in the s -th cell: if $s = 0$, the UE will be termed macrocell user equipments (MUE), and small-cell user equipments (SUE) otherwise, although there is no substantial distinction among the two classes of users, as better clarified in the remainder of this work.

¹For a more detailed description of this assignment mapping, see Section V.

The vector $\mathbf{x}_{k,n} \in \mathbb{C}^{M_{\psi(k)} \times 1}$ collecting the samples received over subcarrier n at the AP serving the k -th UE can then be written as

$$\mathbf{x}_{k,n} = \sum_{j=1}^K \mathbf{h}_{kj,n} \sqrt{p_{j,n} z_{j,n}} + \mathbf{w}_{k,n}, \quad (1)$$

where $\mathbf{w}_{k,n} \sim \mathcal{CN}(\mathbf{0}_{M_{\psi(k)}}, \sigma^2 \mathbf{I}_{M_{\psi(k)}})$ is the background noise in the channel whereas $p_{j,n}$ and $z_{j,n}$ denote the transmit power and data symbol of UE k over subcarrier n respectively. To keep the complexity of the signal processing (SP) at the AP at a tolerable level, a simple linear detection scheme is employed for data detection, although a generalization to nonlinear detectors is straightforward. This means that the entries of $\mathbf{x}_{k,n}$ are linearly combined to form $y_{k,n} = \mathbf{g}_{k,n}^H \mathbf{x}_{k,n}$ where $\mathbf{g}_{k,n}$ is the vector employed for recovering the data transmitted by user k over subcarrier n . The signal-to-interference-plus-noise ratio (SINR) over the n -th subcarrier that is achieved by user k at its serving AP then takes the form:

$$\gamma_{k,n} = \mu_{k,n}(\mathbf{p}_{-k,n}) p_{k,n} \quad (2)$$

where

$$\mu_{k,n}(\mathbf{p}_{-k,n}) = \frac{\|\mathbf{g}_{k,n}^H \mathbf{h}_{kk,n}\|^2}{\|\mathbf{g}_{k,n}\|^2 \sigma^2 + \sum_{j=1, j \neq k}^K \|\mathbf{g}_{k,n}^H \mathbf{h}_{kj,n}\|^2 p_{j,n}} = \frac{\omega_{kk,n}}{\sigma^2 + I_{k,n}} \quad (3)$$

where we have explicitly reported the dependence on $\mathbf{p}_{-k,n} = (p_{1,n}, \dots, p_{k-1,n}, p_{k+1,n}, \dots, p_{K,n})^T$ (the vector collecting all powers transmitted over subcarrier n except that of user k), and we have defined the quantities

$$\omega_{kj,n} = \frac{|\mathbf{g}_{k,n}^H \mathbf{h}_{kj,n}|^2}{\|\mathbf{g}_{k,n}\|^2} \quad (4)$$

and

$$I_{k,n} = \sum_{j \neq k} \omega_{kj,n} p_{j,n}. \quad (5)$$

for a later convenience. Using (2), the achievable rate (normalized to the subcarrier bandwidth, and thus measured in b/s/Hz) of the k -th user will then be:

$$r_k(\mathbf{p}) = \frac{1}{N} \sum_{n=1}^N \log_2 (1 + \gamma_{k,n}), \quad (6)$$

where $\mathbf{p}_k = (p_{k,1}, \dots, p_{k,N})$ denotes the power vector of user k over all subcarriers $n = 1, \dots, N$, and $\mathbf{p} = (\mathbf{p}_1, \dots, \mathbf{p}_K) \in \mathbb{R}_+^{K \times N}$ is the corresponding power profile of all users (obviously, $p_{k,n} = 0$ if user k is not transmitting over subcarrier n). Note that the multiple access interference (MAI) $I_{k,n}$

of user k comes from both intra-cell interference (generated by other UE served by the same AP) and inter-cell interference (from UE served by all other APs). To simplify the notation, the argument of $\mu_{k,n}$ and r_k will be suppressed in what follows.

B. Problem statement

As mentioned in Section I, *energy-efficient* network design must take into account the energy consumption incurred by each UE. To that end, note that in addition to the radiated powers \mathbf{p}_k at the output of the radio-frequency front-end, each terminal k also incurs circuit power consumption during transmission, mostly because of power dissipated at the UE signal amplifier [24, 26]. Therefore, the overall power consumption $P_{T,k}$ of the k -th UE will be given by

$$P_{T,k} = p_{c,k} + P_k = p_{c,k} + \sum_{n=1}^N p_{k,n}, \quad (7)$$

where $P_k = \sum_{n=1}^N p_{k,n}$ is the transmitted power of user k over the entire spectrum, while $p_{c,k}$ represents the average power consumed by the device electronics of the k -th UE (assumed for simplicity to be independent of the transmission state). Following [26, 35], the *energy efficiency* of the link can then be measured (in b/J/Hz) by the utility function

$$u_k(\mathbf{p}) = \frac{r_k}{P_{T,k}} = \frac{N^{-1} \sum_{n=1}^N \log_2 (1 + \mu_{k,n} p_{k,n})}{p_{c,k} + \sum_{n=1}^N p_{k,n}}, \quad (8)$$

where the dependence on the transmit power vectors of all other users is subsumed in the gains $\boldsymbol{\mu}_k = \{\mu_{k,n}\}_{n=1}^N$ of (3). Accordingly, in data-oriented wireless networks, QoS requirements take the form

$$r_k \geq \theta_k, \quad (9)$$

where θ_k is the minimum rate threshold required by user k .

To summarize, the design of an energy-efficient resource allocation scheme which encompasses both subcarrier allocation and power control amounts to the multi-agent, multi-objective optimization problem:

$$\text{maximize } u_k(\mathbf{p}), \quad (10a)$$

$$\text{subject to } N^{-1} \sum_{n=1}^N \log_2 (1 + \mu_{k,n} p_{k,n}) \geq \theta_k, \quad (10b)$$

where $u_k(\mathbf{p})$ is the energy efficiency utility function (8), and (10b) represents the normalized rate requirement (9). Thus, unlike other OFDMA resource allocation problems (see e.g. [36, 37]), subcarrier selection and power loading are tackled in a *joint* manner. Furthermore, inter- and intra-cell interference between UE makes (10) into a game where each UE $k \in \mathcal{K}$ aims at unilaterally maximizing its individual link energy-efficiency via an optimal choice of power allocation vector \mathbf{p}_k – and, in so doing, obviously affects the possible choices of all other UE in the network.

Remark 1. It is easy to see that a particular set of constraints $\{\theta_k\}_{k=1}^K$ may affect the *feasibility* of the problem in the sense that there might not exist *any* power allocation $\mathbf{p} \in \mathbb{R}_+^{K \times N}$ that allows all constraints θ_k to be met *simultaneously* – essentially due to mutual interference in the network which implies a dependence between the gains $\{\mu_{k,n}\}_{n=1}^N$ for all $k = 1, \dots, K$. Providing necessary and sufficient conditions that ensure the feasibility of the problem (10) in the single-carrier case $N = 1$ can be found in [25]. On the other hand, analogous conditions for the general case $N > 1$ subcarriers are very difficult to obtain, and future investigations will focus on addressing this lack.

III. GAME-THEORETIC RESOURCE ALLOCATION

A. Game-theoretic formulation of the problem

As we have already mentioned, the mutual interference in the network introduces an interaction among the users aiming at optimizing their utilities (10). A natural framework for studying such strategic inter-user interactions is offered by the theory of non-cooperative games with continuous (and action-dependent) action sets. Thus, following Debreu [28] (see also [29]), we will formulate the system model of the previous section as a non-cooperative game $\mathcal{G} \equiv \mathcal{G}(\mathcal{K}, \mathcal{P}, u)$ consisting of the following components:

- The set of *players* of \mathcal{G} is the set \mathcal{K} of the network's UE.
- A priori, each player can choose any transmit power vector in $\mathcal{P}_k^0 \equiv \mathbb{R}_+^N$. However, given a power profile $\mathbf{p}_{-k} \in \mathcal{P}_k^0 \equiv \prod_{\ell \neq k} \mathcal{P}_\ell^0$ of the opponents of player k , the *feasible action set* of player k in the presence of the rate requirements (10b) is:

$$\mathcal{P}_k(\mathbf{p}_{-k}) = \left\{ \mathbf{p}_k \in \mathcal{P}_k^0 : r_k(\mathbf{p}) \geq \theta_k \right\}; \quad (11)$$

- The *utility* $u_k(\mathbf{p}_k; \mathbf{p}_{-k})$ of player k is given by (8).

In this framework, the most widely used solution concept is a generalization of the notion of Nash equilibrium [5], known as *Debreu equilibrium* (DE) [28] and sometimes also referred to as a *generalized Nash equilibrium* (GNE) [29]. Formally:

Definition 1. A power profile \mathbf{p}^* is a *Debreu equilibrium* of the energy-efficiency game $\mathcal{G}(\mathcal{K}, \mathcal{P}, u)$ if, for all users $k \in \mathcal{K}$, we have

$$\mathbf{p}_k^* \in \mathcal{P}_k(\mathbf{p}_{-k}^*) \quad (12a)$$

and

$$u_k(\mathbf{p}^*) \geq u_k(\mathbf{p}_k; \mathbf{p}_{-k}^*) \quad \text{for all } \mathbf{p}_k \in \mathcal{P}_k(\mathbf{p}_{-k}^*). \quad (12b)$$

Debreu equilibria are of particular interest in the context of distributed systems because they offer a stable solution of the game from which players (in this case, UE) have no incentive to deviate (and thus destabilize the system) if everyone else maintains their chosen power allocation profiles. Accordingly, in what follows, we investigate the existence and characterization of DE in the energy-efficient power allocation game \mathcal{G} , leaving the question of uniqueness and convergence to such states to Sections III-C and IV, respectively.

B. Problem feasibility and equilibrium existence

Debreu's original analysis [28] provides a general equilibrium existence result under the following assumptions:

- (D1) The players' feasible action sets $\mathcal{P}_k(\mathbf{p}_{-k})$ are nonempty, closed, convex, and contained in some compact set \mathcal{C}_k for all $\mathbf{p}_{-k} \in \mathcal{P}_{-k} \equiv \prod_{\ell \neq k} \mathcal{P}_\ell$.
- (D2) The sets $\mathcal{P}_k(\mathbf{p}_{-k})$ vary continuously with \mathbf{p}_{-k} (in the sense that the graph of the set-valued correspondence $\mathbf{p}_{-k} \mapsto \mathcal{P}_k(\mathbf{p}_{-k})$ is closed).
- (D3) Each user's payoff function $u_k(\mathbf{p}_k; \mathbf{p}_{-k})$ is quasi-concave in \mathbf{p}_k for all $\mathbf{p}_{-k} \in \mathcal{P}_{-k}$.

In our setting, the Shannon rate function $r_k(\mathbf{p}_k; \mathbf{p}_{-k})$ of (6) is concave in \mathbf{p}_k and unbounded from above, so $\mathcal{P}_k(\mathbf{p}_{-k})$ is convex and nonempty for all $\mathbf{p}_{-k} \in \mathcal{P}_{-k}^0$. Moreover, $\mathcal{P}_k(\mathbf{p}_{-k})$ varies continuously with \mathbf{p}_{-k} because the constraints (10b) are themselves continuous in \mathbf{p}_{-k} . Finally, it is easy to show that $u_k(\mathbf{p}_k; \mathbf{p}_{-k})$ is quasi-concave in \mathbf{p}_k : since $u_k(\mathbf{p}_k; \mathbf{p}_{-k}) \geq a$ if and only if

$$r_k(\mathbf{p}_k; \mathbf{p}_{-k}) - a \left(p_c + \sum_{n=1}^N p_{k,n} \right) \geq 0, \quad (13)$$

and since the set defined by this inequality is convex for every $\mathbf{p}_{-k} \in \mathcal{P}_{-k}$ (recall that r_k is concave in \mathbf{p}_k), quasi-concavity of $u_k(\cdot, \mathbf{p}_{-k})$ follows.

Unfortunately however, even though the users' best response sets

$$\mathcal{P}_k^*(\mathbf{p}_{-k}) \equiv \arg \max_{\mathbf{p}_k \in \mathcal{P}_k(\mathbf{p}_{-k})} u_k(\mathbf{p}_k; \mathbf{p}_{-k}) \quad (14)$$

are easily seen to be nonempty, convex, closed and bounded for every \mathbf{p}_{-k} , they might (and typically do) run off to infinity – i.e. they are not *uniformly* bounded. To understand this, simply consider the case of two UE transmitting over a single channel: if one of the UE transmits at very high power, the other UE is forced to transmit at a commensurately high power in order to meet its rate requirement. This leads to a cascade of power increases that makes each UE's feasible action set $\mathcal{P}_k(\mathbf{p}_{-k})$ (and, hence, $\mathcal{P}_k^*(\mathbf{p}_{-k})$ as well) escape to infinity as the other UE increases its individual power. Formally, this means that the UE' feasible action sets $\mathcal{P}_k(\mathbf{p}_{-k})$ are not contained in an enveloping bounded set \mathcal{C}_k , so Debreu's equilibrium existence theorem [28] does not apply.

From a power control perspective, this is not surprising: as is well known [38], the problem (10) may fail to be feasible, i.e. there may be no power profile $\mathbf{p} = (\mathbf{p}_1, \dots, \mathbf{p}_K)$ such that $\mathbf{p}_k \in \mathcal{P}_k(\mathbf{p}_{-k})$ for all k . Obviously, in this case, the energy-efficiency game \mathcal{G} does not admit an equilibrium either. On the other hand, at a purely formal level, equilibrium existence and problem feasibility are restored if we assume that users can transmit with infinitely high power, i.e. each UE $k \in \mathcal{K}$ chooses its total transmit power from the compactified half-line $[0, +\infty]$. In this extended setup, there are two points where indeterminacies may arise: first, the utility of player k is not well-defined if $p_{k,n} = +\infty$ for some n ; second, the rate requirement (10b) of user k is also ill-defined if $p_{\ell,n} = +\infty$ for some $\ell \neq k$. To address these problems, note first that the utility function (8) of player k decreases to 0 when $p_{k,n} \rightarrow +\infty$ for some channel $n = 1, \dots, N$, reflecting the fact that $\lim_{x \rightarrow +\infty} x^{-1} \log_2 x = 0$. Thus, by continuity, the utility of player k for infinite transmit powers $p_{k,n}$ may be defined as:

$$u_k(\mathbf{p}) = 0 \quad \text{whenever } p_{k,n} = +\infty \text{ for some } n. \quad (15)$$

As for the rate requirements of user k , a simple exponentiation of (10b) for finite p yields the equivalent expression:

$$\prod_{n=1}^N (1 + \mu_{k,n} p_{k,n}) \geq 2^{N\theta_k} \quad (16)$$

or, after substituting for $\mu_{k,n}$ and rearranging:

$$\prod_{n=1}^N \left(\|\mathbf{g}_{k,n}\|^2 \sigma^2 + \sum_{j=1}^K |\mathbf{g}_{k,n}^H \mathbf{h}_{kj,n}|^2 p_{j,n} \right) \geq 2^{N\theta_k} \prod_{n=1}^N \left(\|\mathbf{g}_{k,n}\|^2 \sigma^2 + \sum_{j \neq k} |\mathbf{g}_{k,n}^H \mathbf{h}_{kj,n}|^2 p_{j,n} \right). \quad (17)$$

Since both sides of (17) are well-defined for all $p_{j,n} \in [0, +\infty]$, (17) provides a reformulation of (10b) that remains meaningful even in the extended arithmetic of $[0, +\infty]$.

In this infinite-power framework, any power profile $\mathbf{p}^* = (\mathbf{p}_1^*, \dots, \mathbf{p}_K^*)$ with $\sum_{n=1}^N p_{k,n}^* = +\infty$ for all $k \in \mathcal{K}$ is feasible with respect to (17). Furthermore, if player k deviates *unilaterally* and starts transmitting with finite total power, its rate requirement (17) will be automatically violated and its utility equals 0. Consequently, no player can gain a utility greater than 0 by deviating from \mathbf{p}^* . This shows that the resulting infinite-power game $\bar{\mathcal{G}}$ with utility functions and rate requirements extended as in (15) and (17) above always admits a DE – and trivially so. However, any such equilibrium is clearly unreasonable from a practical standpoint as it represents a cascade of power increases that escapes to infinity as players try to meet their power constraints. Therefore, in what follows, we will focus on conditions and scenarios which guarantee that:

- 1) The energy-efficiency game \mathcal{G} admits a DE with finite transmit powers (Section III-C).
- 2) The equilibrium is unique (Section III-C).
- 3) Users converge to this equilibrium by following an adaptive, distributed algorithm (Section IV).

C. Equilibrium characterization and uniqueness

In this section, our goal is to characterize the game's DE by exploiting the fact that they are the fixed points of a certain best-response mapping.

Proposition 1. *A transmit power profile \mathbf{p} is at Debreu equilibrium if and only if its components $p_{k,n}^*$ satisfy:*

$$p_{k,n}^* = \left(\frac{1}{\lambda_k^*} - \frac{1}{\mu_{k,n}} \right)^+ \quad (18)$$

where

$$\lambda_k^* = \min \{ \lambda_k, \bar{\lambda}_k \}. \quad (19)$$

In the above,

$$\lambda_k = \frac{W(\alpha_k \cdot e^{\beta_k - 1})}{\alpha_k} \quad (20)$$

is the water level of the water-filling operator (18) when the problem (10) is solved without the minimum-rate constraints (10b) (i.e. when $\theta_k = 0$ for all $k \in \mathcal{K}$), $W(\cdot)$ denotes the Lambert W function [34], while

$$\alpha_k = |\mathcal{S}_k|^{-1} \left(p_{c,k} - \sum_{n \in \mathcal{S}_k} \mu_{k,n}^{-1} \right) \quad (21)$$

and

$$\beta_k = |\mathcal{S}_k|^{-1} \sum_{n \in \mathcal{S}_k} \ln \mu_{k,n} \quad (22)$$

where $\mathcal{S}_k = \{n \in \mathcal{N} : \mu_{k,n} \geq \lambda_k\}$ denotes the subset of active subcarriers when using the uncoded energy-efficient formulation. Similarly:

$$\bar{\lambda}_k = \left(2^{-N\theta_k} \prod_{n \in \bar{\mathcal{S}}_k} \mu_{k,n} \right)^{1/\bar{\mathcal{S}}_k} \quad (23)$$

is the water level of (18) when all minimum-rate constraints (10b) are met simultaneously with equality (i.e. (10) reduces to a power minimization problem with equality rate constraints $r_k = \theta_k$), and, as above, $\bar{\mathcal{S}}_k = \{n \in \mathcal{N} : \mu_{k,n} \geq \bar{\lambda}_k\}$ denotes the subset of active subcarriers under this formulation.

Proof: The proof is given in Appendix A and relies on defining the best-response mapping and using fractional programming to characterize its fixed points. ■

Remark 2. Proposition 1 does not provide a way to calculate the water levels λ_k and $\bar{\lambda}_k$. For an iterative computational method, the reader is instead referred to Section IV.

In spite of its tedious appearance, Proposition 1 is of critical importance both from a theoretical and practical point of view. Indeed, it is the basic step which allows us to derive sufficient conditions ensuring the existence and uniqueness of the DE and also to develop a distributed and scalable power allocation algorithm which steers the network to a stable equilibrium state.

To that end, note that the equilibrium characterization of Proposition 1 may be vacuous if the game does not admit a DE to begin with – for instance, if the original power control problem is not feasible. On the other hand, if the game \mathcal{G} does admit a DE, then this DE might not be unique – just as in the analysis of [31]. The next proposition provides a sufficient condition for the users' best response correspondence to be a contraction mapping, thus ensuring the existence and uniqueness of a DE for \mathcal{G} .

Proposition 2. *The energy-efficiency game \mathcal{G} admits a unique DE \mathbf{p}^* whenever, for all users $k \in \mathcal{K}$, we have:*

$$\sum_{j=1}^K \sum_{\substack{n=1 \\ j \neq k}}^N \omega_{kj,n}^2 \cdot \sup_{\boldsymbol{\mu}_k \in \Omega_k} \left[\frac{1}{\varsigma_k^*} \sum_{n \in \mathcal{S}_k^*} \omega_{kk,n}^{-2} (\xi_{k,n}^2 + \varsigma_k^* - 2\xi_{k,n}) \right] < 1, \quad (24)$$

where $\Omega_k = \prod_{n=1}^N (0, \sigma^{-2} \omega_{kk,n}]$, $\varsigma_k^* = |\mathcal{S}_k^*|$, and

$$\mathcal{S}_k^* = \begin{cases} \bar{\mathcal{S}}_k & \text{if } \lambda_k \geq \bar{\lambda}_k \\ \mathcal{S}_k & \text{if } \lambda_k < \bar{\lambda}_k \end{cases} \quad (25)$$

$$\xi_{k,n} = \begin{cases} \mu_{k,n} \bar{\lambda}_k^{-1} & \text{if } \bar{\lambda}_k \leq \lambda_k \text{ and } n \in \mathcal{S}_k^*, \\ \frac{\mu_{k,n} - \lambda_k}{\lambda_k(1+\nu_k)} & \text{if } \bar{\lambda}_k > \lambda_k \text{ and } n \in \mathcal{S}_k^*, \\ 0, & \text{if } n \notin \mathcal{S}_k^*, \end{cases} \quad (26)$$

with

$$\nu_k = -\ln \lambda_k + (\beta_k - 1). \quad (27)$$

Proof: The main steps for the proof are given in Appendices B and C; for a more detailed version, the reader is referred to the online technical report [39]. ■

Remark 3. Notice that these sufficient conditions are similar to the well-known conditions ensuring the uniqueness of a Nash equilibrium in the rate maximization non-cooperative game for interference channels [40]. Intuitively, (24) means that, if the interfering communications for a user are sufficiently far away and the resulting SINR is high enough, then the DE exists and is unique. However, these conditions include a non-trivial optimization step w.r.t. μ_k . Indeed, the variables of the problem impact the values of λ_k^* , \mathcal{S}_k^* and all functions $\xi_{k,n}$, making the conditions rather difficult to be exploited.

To tackle this issue, the online technical report [39] provides a set of sufficient conditions that are simpler, because they depend only on the system parameters by upper-bounding the supremum term in (24). The downside is that these simple conditions are more stringent than (24). Nevertheless, it is worth stressing that the users of the network are never required to compute these conditions: they are only meant as a safety feature to guard against catastrophic system instabilities, to be calculated by the network administrator based on expected network usage scenarios.

Remark 4. Since the conditions of Proposition 2 are only sufficient, DE might exist even in the case where (24) does not hold for some $k \in \mathcal{K}$. As a matter of fact, when problem (10) is feasible, the distributed algorithm that we present in Section IV was observed to converge to a DE in all the numerical simulations performed and for every network scenario considered, some of which are illustrated in Section V.

Algorithm 1 Iterative algorithm to solve problem (10).

```

set  $t = 0$ .
initialize  $\mathbf{p}_k[t] = \mathbf{0}_N$  for all users  $k \in \mathcal{K}$ 
repeat
  for  $k = 1$  to  $K$  do
    {loop over the users}
    receive  $\{\gamma_{k,n}[t]\}_{n=1}^N$  from the serving AP
    compute  $\lambda_k$  using Algorithm 2 and  $\bar{\lambda}_k$  using inverse water-filling
    set  $\lambda_k^* = \min\{\lambda_k, \bar{\lambda}_k\}$ 
    for  $n = 1$  to  $N$  do
      {loop over the carriers}
      update  $p_{k,n}[t + 1] = (1/\lambda_k^* - p_{k,n}[t]/\gamma_{k,n}[t])^+$ 
    end for
  end for
  update  $t = t + 1$ 
until  $\mathbf{p}_k[t] = \mathbf{p}_k[t - 1]$  for all  $k \in \mathcal{K}$ 

```

IV. DISTRIBUTED IMPLEMENTATION

To derive a practical procedure allowing UE to reach the DE of \mathcal{G} in a distributed fashion (*without* any distinction between SUE and MUE), we start by focusing on a specific UE $k \in \mathcal{K}$ and assume that all other UE $j \neq k$ have already chosen their optimal transmit powers $\mathbf{p}_{-k} = \mathbf{p}_{-k}^*$ (in a possibly asynchronous fashion). From (3), we then see that the gains $\mu_{k,n}(\mathbf{p}_{-k,n}^*)$ needed to implement (18) are simply

$$\mu_{k,n}(\mathbf{p}_{-k,n}^*) = \frac{\gamma_{k,n}}{p_{k,n}} \quad (28)$$

for all $n \in \mathcal{N}$. This means that the only information that is not locally available at the k -th UE to compute the optimal powers $\{p_{k,n}^*\}$ is the set of SINRs $\{\gamma_{k,n}\}$ measured at UE k 's serving SCA, and which can be sent with a modest feedback rate requirement on the return channel (a discussion on the impact of a limited feedback can be adapted to this specific scenario from [41]).

Based on the above considerations, we can derive an iterative and fully decentralized algorithm to be adopted by each UE k at each time step t to solve the fixed-point system of equations (18) with a low-complexity, scalable and adaptive procedure. The pseudocode for the whole network is

Algorithm 2 Iterative algorithm to compute λ_k as in (20).

```

set a tolerance  $\varepsilon \ll 1$ 
{initialization of the Dinkelbach method:}

repeat
  select a random  $\lambda_k \in \mathbb{R}$ 
  for  $n = 1$  to  $N$  do
    set  $p_{k,n} = (1/\lambda_k - p_{k,n}[t]/\gamma_{k,n}[t])^+$ 
  end for
  compute  $\varphi(\mathbf{p}_k)$  using (31) and  $\chi(\mathbf{p}_k)$  using (32) (see Appendix A)
  set  $\Phi(\lambda_k) = \varphi(\mathbf{p}_k) - \lambda_k \chi(\mathbf{p}_k)$ 
  until  $\Phi(\lambda_k) \geq 0$ 
{Dinkelbach method:}

while  $\Phi(\lambda_k) \geq \varepsilon$  do
  set  $\lambda_k = \varphi(\mathbf{p}_k)/\chi(\mathbf{p}_k)$ 
  for  $n = 1$  to  $N$  do
    set  $p_{k,n} = (1/\lambda_k - p_{k,n}[t]/\gamma_{k,n}[t])^+$ 
  end for
  update  $\varphi(\mathbf{p}_k)$  using (31) and  $\chi(\mathbf{p}_k)$  using (32)
  set  $\Phi(\lambda_k) = \varphi(\mathbf{p}_k) - \lambda_k \chi(\mathbf{p}_k)$ 
end while

```

summarized in Algorithm 1. Note that, in practice, each UE $k \in \mathcal{K}$ only needs to implement the steps for only one value in the (i.e., his own index) loop over the users, so the algorithm is suitable for an asynchronous implementation and a dynamic network configuration, where each UE only requires the SINRs fed back by the serving SCA, without any further information on the network.

For the sake of clarity, the algorithm to compute λ_k for each UE $k \in \mathcal{K}$ as in (20) is reported in Algorithm 2, whereas $\bar{\lambda}_k$ can easily be computed using standard inverse water-filling (IWF) algorithms (e.g., see [30]). Note that, although (20) is derived analytically in closed form and can be computed directly, it is still appealing to use the iterative procedure outlined in Algorithm 2 which takes advantage of the Dinkelbach approach [42] based on Newton's method. This numerical method significantly reduces the computational complexity of evaluating the Lambert W function.

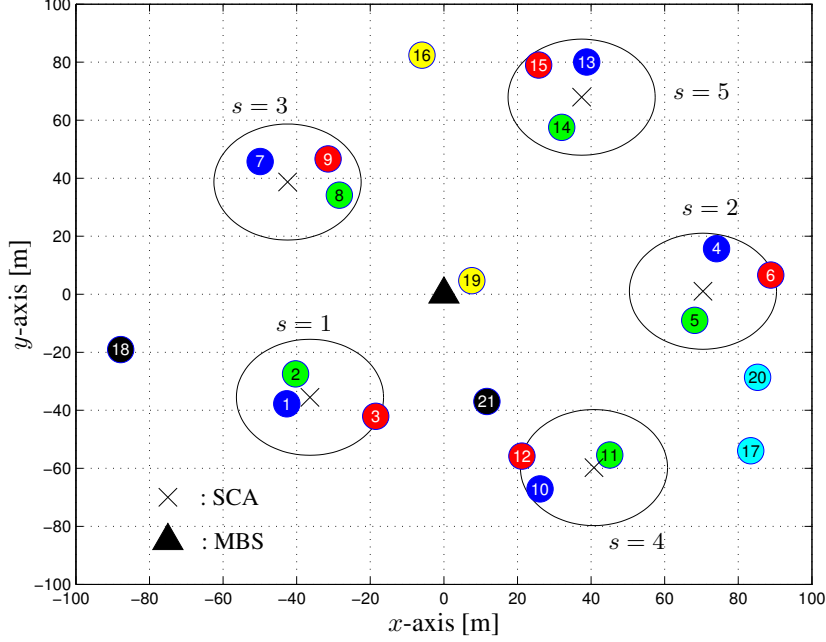


Fig. 1. Random realization of a network with $S = 5$ small cells, $K_S = 3$ SUE, and $K_0 = 6$ MUE, sharing $N = 12$ subcarriers.

For the sake of brevity, Algorithm 2 makes use of some functions which we will introduce in the proof of Proposition 1. For future reference, throughout the simulations reported in Section V, the convergence tolerance is set to $\varepsilon = 10^{-5}$ and we check whether the end state of the algorithm is a DE by testing the characterization of Proposition 1.

Proposition 3. *The iterates of Algorithm 1 converge to the Debreu equilibrium whenever (24) holds.*

Proof: The convergence of Algorithm 1 to the equilibrium point follows from the contraction properties of the best-response mapping investigated in Section III-C. ■

Remark 5. Although the contraction properties of the best-response mapping are contingent on the sufficient conditions of Proposition 2 to hold, Algorithm 1 is still seen to converge to a DE of \mathcal{G} , provided that the problem is feasible to begin with (please see the next section for a numerical assessment by means of extensive numerical simulations).

V. SIMULATION RESULTS

In this section, our aim is to evaluate the performance of the proposed algorithm under different operating conditions via numerical simulations. To keep the complexity of the simulations tractable

Table I
GENERAL SYSTEM PARAMETERS

Parameter	Value	Parameter	Value
Bandwidth	$B = 11.2 \text{ MHz}$	Carrier spacing	$\Delta f = 10.9375 \text{ kHz}$
Carrier frequency	$f_c = 2.4 \text{ GHz}$	Macro-cell area	0.04 km^2
Total number of small cells	$S = 5$	Small-cell radius	$\rho_S = 20 \text{ m}$
Number of antennas (MBS, SCA)	$M_0 = 16, M_S = 4$	Density of population	$1,000 \text{ users/km}^2$
Number of SUE per small cell	$K_S = 4$	Number of MUE	$K_0 = 20$
Number of subcarriers	$N = 96$	Noise power	$B\sigma^2 = -103.3 \text{ dBm}$
Non-radiative power	$p_c = 20 \text{ dBm}$	Path-loss exponent	$\zeta = 3.5$
Cut-off parameter	$d_{\text{ref}} = 35 \text{ m}$	Average path-loss attenuation at d_{ref}	$L_{\text{ref}} = -84.0 \text{ dB}$

while considering a significantly loaded system, we focus on the scenario reported in Fig. 1, where a squared macrocell over an area of $200 \times 200 \text{ m}^2$, with its macrocell base station (MBS) placed at its center, accommodates S randomly distributed small cells, each having a radius $\rho_s = \rho_S = 20 \text{ m}$. Throughout the simulations, unless otherwise specified, we adopt the parameters reported in Table I (see [24] and references therein), where, for simplicity, each SC is assumed to have the same number of antennas M_S and users K_S , and all UE are assumed to have the same non-radiative power consumption $p_{c,k} = p_c$. To include the effects of fading and shadowing into our simulations, we use the path-loss model introduced in [43, 44], using a 24-tap channel model to reproduce multipath effects. For simplicity, we also assume perfect channel estimation at the receiver end and the use of maximum ratio combining (MRC) techniques, which amounts to setting $\mathbf{g}_{k,n} = \mathbf{h}_{k,n}$ for all $k \in \mathcal{K}$ and $n \in \mathcal{N}$. The UE $k \in \mathcal{K}$ is then assigned to APs $s \in \mathcal{S}$ following the mapping:

$$\psi(k) = \begin{cases} s, & \exists s > 0 \text{ s.t. } d_{k,s} \leq \rho_S, \\ 0, & \text{otherwise,} \end{cases} \quad (29)$$

where $d_{k,s}$ denotes the distance between UE k and SCA s . Without loss of generality, we will measure the performance for a specific user (say user 1) within either a small cell or a macrocell, by averaging over all possible positions of the users, uniformly randomizing their minimum-rate constraints θ_k in $[0, 2] \text{ [b/s/Hz]}$ for $k \neq 1$.

To evaluate the proposed algorithm in a practical setting, Fig. 1 reports a random realization of the network with the parameters described above, in which the following quantities have been reduced for the sake of graphical representation: $K_S = 3$, $K_0 = 6$, and $N = 12$, $\theta_k = 1.5 \text{ b/s/Hz}$ for SUE, and $\theta_k = 0.5 \text{ b/s/Hz}$ for MUE. Using the distributed algorithm described in Section IV, after

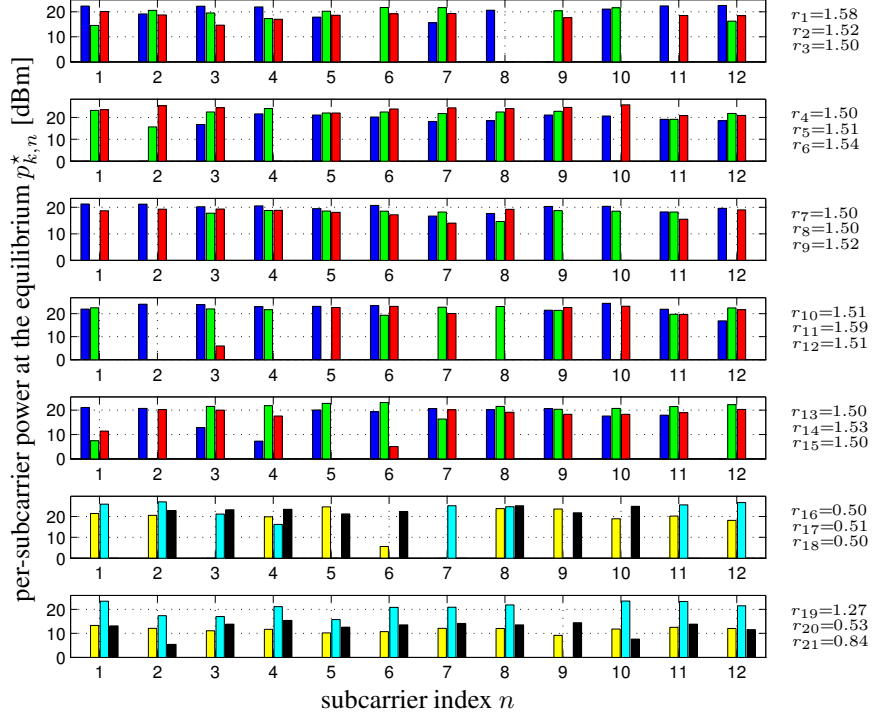


Fig. 2. Outcome of the resource allocation for the scenario of Fig. 1. The subcarriers are allocated exclusively when the MAI within the small cell is large. All users achieve their rate requirements. Users with favorable channels increase their powers to maximize their own utilities.

16 iterations we get the solution to (10), representing the users' power profile at the DE of \mathcal{G} , and reported in Fig. 2. Here, the first five subplots correspond to the powers allocated in the small cells (the s th subplot depicts the powers allocated by the users in the s th small cell, with colors matching the ones used in Fig. 1), whereas the last two subplots show the powers selected by the MUE labeled $\{16, 17, 18\}$ (in the sixth subplot) and $\{19, 20, 21\}$ (in the seventh subplot), respectively. As can be seen in Fig. 2, this method tends to allocate the subcarriers in an exclusive manner whenever the MAI across UE within the same small cell is too large (e.g., see the 4th small cell, in which only 5 subcarriers are shared by the 3 users), and to share the same subcarrier when the MAI across users is at a tolerable level (which also includes the interference generated by SUE from neighboring cells and the MUE). On the right hand side, we report the achieved rates at the DE in b/s/Hz. As can be verified, all users achieve their minimum demands, while for users with particularly favorable channel conditions (in this case, users no. 1, 11, 19, and 21), it is convenient to increase their transmit power so as to obtain better performance in terms of EE.

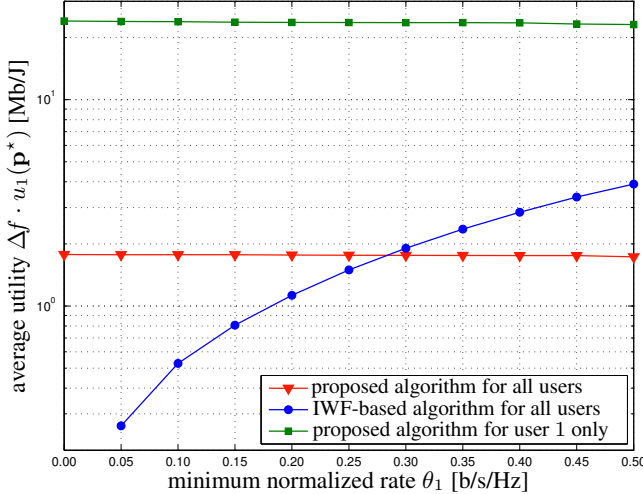


Fig. 3. Average utility at the equilibrium as a function of the minimum rate θ_1 . Compared to an IWF-based solution, the Debreu equilibrium may perform worse in terms of overall network utility. However, the IWF-based solution is not a stable operating point: user 1 has always an incentive to deviate and highly increase its own utility.

To the best of our knowledge, there are no resource allocation algorithms that address the energy-efficient formulation (10) subject to the minimum-rate demands (10b). To evaluate the improvement in terms of EE of the proposed technique (red line), we thus compare its performance with that achieved by an IWF-based solution (blue line), in which all users aim at meeting θ_k with equality. Fig. 3 reports the average utility achieved by averaging over all possible positions of a particular MUE (say user 1) as a function of a specific minimum rate θ_1 , using the parameters reported in Table I.² Interestingly, there exists a critical θ_1 (in this case, 0.28 b/s/Hz), for which the EE of IWF is higher than that achieved by the proposed formulation, mainly due to a weaker MAI caused by the IWF users, that transmit at lower powers than energy-efficient ones (not reported for the sake of brevity). However, the IWF is *not* stable: if the network's UE adopt an IWF approach, then a UE that deviates from this criterion would stand to gain *a much higher EE utility* (represented by the green line in Fig. 3). This situation is reminiscent of the well-known prisoner's dilemma [5] where there exist states with higher average utility, but which are obviously abandoned once a user deviates in order to maximize his individual benefits – and, hence, are inherently unstable in a non-cooperative, decentralized setting. In addition to this, the proposed approach shows two interesting properties

²Throughout all the simulations in the present and subsequent graphs, the selected parameters yield an occurrence of feasible scenarios, assessed a posteriori by letting each UE achieve their minimum-rate constraint (10b) with equality, larger than 99%. Once the scenario is checked to be feasible, the convergence of Algorithm 1 to a stationary point (a DE) occurs with probability 1.

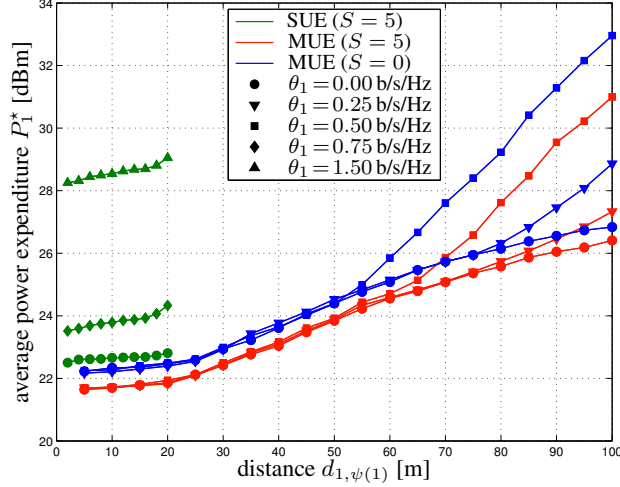


Fig. 4. Average transmit power at the equilibrium as a function of the distance from the receiver. The HetNet configuration ($S = 5$) significantly reduces the power consumption of the UE compared to the macro-cell classical scenario ($S = 0$) for any rate requirements.

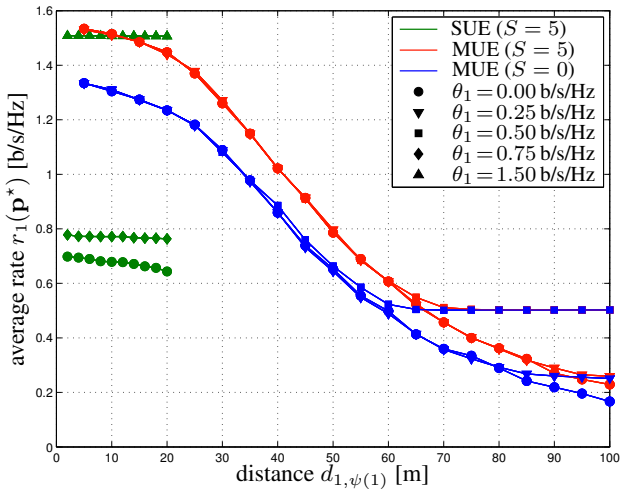


Fig. 5. Average rate at the equilibrium as a function of the distance from the receiver. The HetNet configuration ($S = 5$) significantly increases the rates of the UE compared to the macro-cell classical scenario ($S = 0$) for any rate requirements.

compared to IWF: *i*) averaging over all network realizations and all minimum rates, Algorithm 1 achieves an average utility of 1.76 Mb/J, which is larger than the IWF-based one, equal to 1.69 Mb/J; and *ii*) it introduces fairness among the users, as its performance in terms of EE is weakly dependent on the QoS requirement θ_k .

To measure the benefits of a HetNet configuration with respect to a classical macrocellular architecture ($S = 0$), Figs. 4 and 5 depict the average total transmit powers and the achievable rates at equilibrium in terms of the distance between the observed user and its receiver, averaged over 2,000 independent feasible network realizations per marker. The green and red lines represent the performance in the case of $S = 5$ small cells, $K_S = 4$ SUE, and $K_0 = 20$ MUE, achieved by an SUE and an MUE, respectively, whereas blue lines show the performance obtained by an MUE in the case $S = 0$. We consider three different minimum demands for the SUE (0, 0.75, and 1.5 b/s/Hz, represented by circular, square, and upward-pointing arrowheads), and three different demands for the MUE (0, 0.25, and 0.5 b/s/Hz, represented by circular, downward-pointing arrowheads, and diamond markers respectively). As can be seen, the HetNet configuration introduces *significant gains in both the achievable rates and the power consumption* compared to the classical scenario: by averaging over all possible positions of SUE and MUE across the macrocell area, MUE get $r_1(\mathbf{p}^*) \approx 0.68$ b/s/Hz

with a power consumption $P_1^* \approx 27.5$ dBm (566 mW) when placing $\theta_1 = 0.5$ b/s/Hz,³ compared to $r_1(\mathbf{p}^*) \approx 0.63$ b/s/Hz with $P_1^* \approx 29.1$ dBm (813 mW) for the same minimum demand in the case $S = 0$. The HetNet configuration is also *beneficial in terms of ASE*: using these parameters, we get on average slightly more than 600 b/s/Hz/km², compared to 500 b/s/Hz/km² with $S = 0$.

Introducing small cells has a negative impact in terms of convergence speed of the algorithm: here, on average 4.1 iterations are required for the case $S = 5$, compared to 3.5 for the case $S = 0$. This is due to decentralizing the resource allocation at each receiving station, thus slightly slowing the convergence of the algorithm. However, this provides a better MAI management ensured by SCAs, that allow SUE to obtain *higher rates with lower interfering powers* at the MBS. As can be seen, due to the path-loss model employed, which is roughly constant for distances within $d_{\text{ref}} > \rho_S$, the SUE performance is *independent of the distance from the SCA*. When SUE place $\theta_1 = 1.5$ b/s/Hz, the spectral efficiency is similar to that achieved by MUE located at comparable distance from the MBS (see Fig. 5), but at the cost of a larger power consumption (see Fig. 4): this is due to a better diversity at the receiver obtained by the MUE, since the MBS employes a larger number of antennas (16 versus 4). However, this does not hold true anymore as the MUE distance increases: averaging over all positions, SUE obtain an average rate $r_1(\mathbf{p}^*) \approx 1.51$ b/s/Hz (more than twice the MUE's one) using $P_1^* \approx 28.6$ dBm (732 mW, slightly higher than the MUE's one).

To emphasize the impact of small cells on the system performance, Figs. 6 and 7 compare the performance, averaged over 10^5 independent network realizations, achieved by an MUE using $\theta_1 = 0.25$ b/s/Hz in the same network as before, populated by $K = 40$ users, as a function of the number of SCs S , each having $K_S = 4$ SUE, ranging from $S = 0$ (classical macrocell) to $S = 10$ (only SCs – in this case, the MUE of interest becomes an SUE). Fig. 6 depicts the achievable rate (red line, left axis) and the total power consumption (blue line, right axis), whereas Fig. 7 shows the ASE. As is apparent, introducing SCs in the system has a *significant benefit in terms of all performance indicators*. Of course, this comparison does not account for the additional complexity and drawbacks introduced by increasing S (to mention a few, initial cost of network deployment and maintenance, and complexity of the system). However, although a suitable tradeoff needs to be sought, our analysis confirms that *network densification is one of the key factors to meet 5G requirements* [46].

To verify the scalability of the proposed resource allocation algorithm, we also investigate the

³Note that such minimum demand is about one order of magnitude larger than the one considered for cell-edge users in 4G networks, equal to 0.07 b/s/Hz [45] for a scarcely populated cell (at most 10 users).

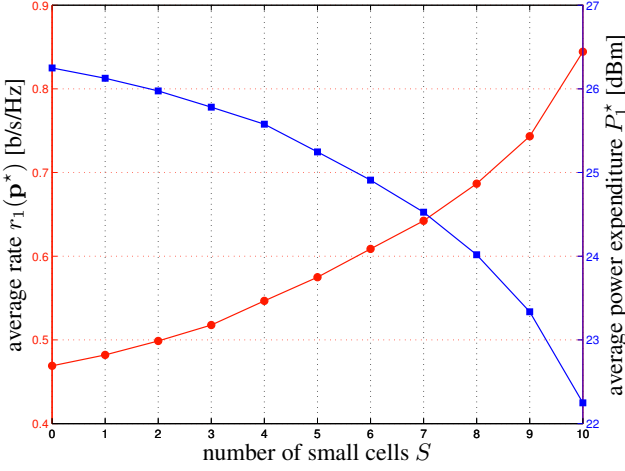


Fig. 6. Average rate at the equilibrium (left axis) and average power consumption (right axis) as functions of the number of small cells. Introducing more small cells increases the average rate and reduces the average power consumption in the network while guaranteeing the minimum rate requirements.

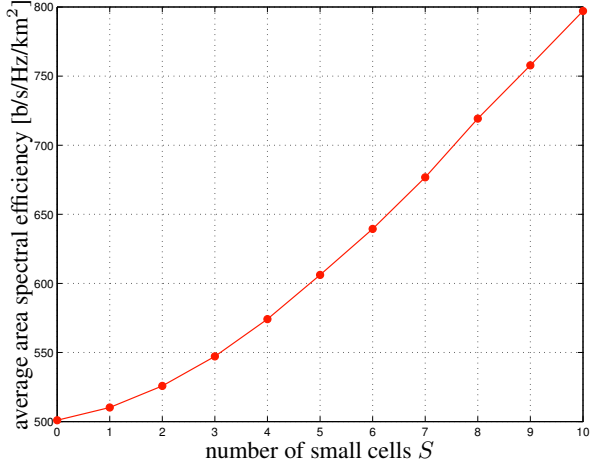


Fig. 7. Average area spectral efficiency as a function of the number of small cells. Introducing more small cells increases the average area spectral efficiency as well.

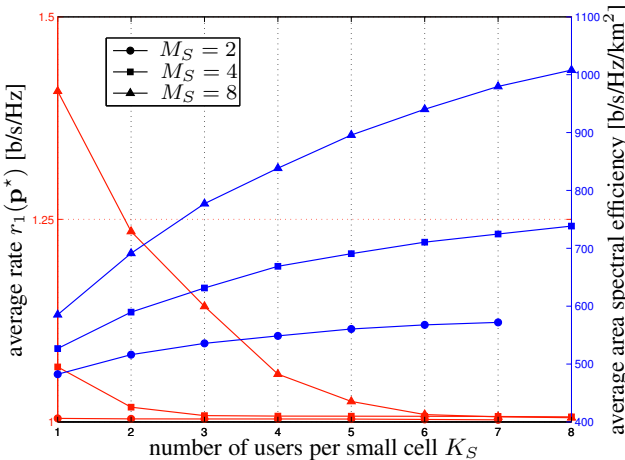


Fig. 8. Average rate (left axis) and average ASE (right axis) as functions of the number user per small cell. The average rate decreases with the number of users per small cell because of the MAI. However, the ASE is increasing with the the number of users per small cell. Moreover, increasing the number of receiving antennas at the SCA improves both, the average rate and average ASE.

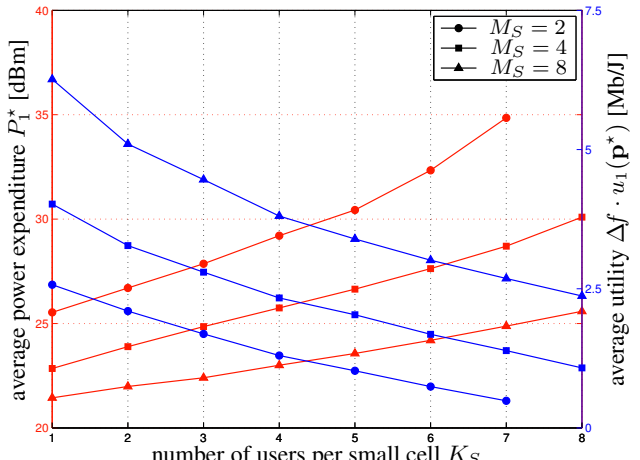


Fig. 9. Average power consumption (left axis) and average utility $\Delta f \cdot u_1(p^*)$ [Mb/J] as functions of the number user per small cell. The average power expenditure is increasing with the number of users per small cells. Given the negative effects on the rate, the average EE is decreasing with the number of users per small cells. Increasing the number of receiving antennas at the SCA improves both the average power expenditure and EE.

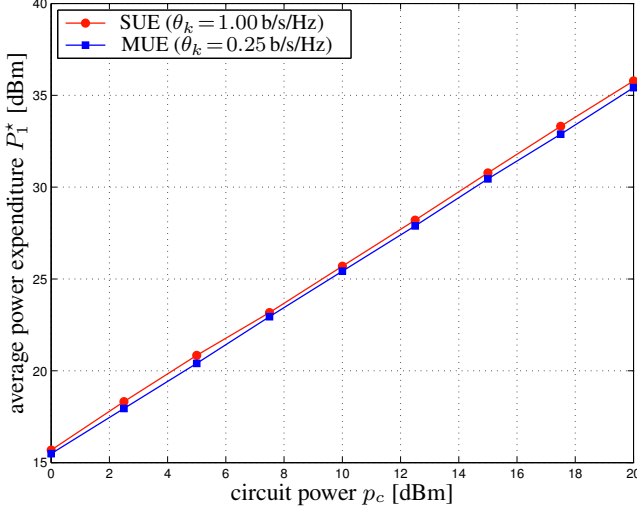


Fig. 10. Average power at the equilibrium as a function of the circuit power. The average power consumption scales linearly with the circuit power in the EE formulation.

impact of the number of receiving antennas at the SCA M_S . In Fig. 8, we plot the spectral efficiency (red lines, left axis) and the ASE (blue lines, right axis) as a function of the number of users per small cell K_S . Similarly, in Fig. 9, we report the power consumption (red lines, left axis) and the utility (blue lines, right axis) versus K_S . Circular, squared, and triangular markers represent the cases for $M_S = \{2, 4, 8\}$ antennas at the SCA. The ASE is averaged over all users $K = K_0 + S \cdot K_S$, whereas the achievable rate is computed for an SUE of interest using $\theta_1 = 1$ b/s/Hz, averaging over 10^5 independent network realizations. As can be seen, increasing the number of antennas yields significant performance gains, thus representing a design parameter that should be highly exploited to boost the performance. Not only the spectral efficiency, as expected, benefits from increasing M_S (as an example, we can move from 500 b/s/Hz/km², achieved when using 2 antennas, to 1,000 b/s/Hz/km², by increasing the number of receiving antennas up to 8, supporting $K = 60$ users), but *also does the EE*, confirming a recent result available in [47]: here, when $K_S = 7$, moving from $M_S = 2$ to 8 yields more than a 5-fold increase in the utility.

Finally, to evaluate the impact of the circuit power p_c on the EE of the system, we report in Fig. 10 the performance of the proposed algorithm as a function of p_c , averaged over 10^5 independent network realizations, where the red line refers to an SUE using $\theta_k = 1$ b/s/Hz, and the blue line refers to an MUE using $\theta_k = 0.25$ b/s/Hz. For all selected non-radiative powers $p_c \in [0, 20]$ dBm, the hypothesis $p_c \gg \sigma^2$ holds, which is in line with the state of the art for radio-frequency and baseband transceiver modeling [24]. As can be seen, the total power consumption at the equilibrium $P_1(\mathbf{p}^*)$ is

directly proportional to p_c . Put differently, the energy-efficient equilibrium point is highly impacted by the non-radiative power, and the bit-per-Joule metric suggests the use a radiative power which is comparable with the non-radiative one. Interestingly, the (normalized) achievable rates at equilibrium (not reported for concision) do not depend on p_c (1.1 and 0.6 b/s/Hz for SUE and MUE, respectively). This confirms a result which is well-known in the literature (e.g., see [26, 48]): *EE increases as the circuit (non-radiative) power decreases*. Hence, reducing p_c , which is one of the main drivers in the device design further boosting the research in this field, can achieve a two-fold goal: not only is it expedient to reduce the constant power consumption (from an electronics point of view), but also it leads energy-aware terminals to reduce their radiative power when they aim at maximizing their bit-per-Joule performance (from an information-theoretic and resource-allocation perspective).

VI. CONCLUSIONS AND PERSPECTIVES

In this paper, we proposed a distributed power allocation scheme for energy-aware, non-cooperative wireless users with minimum-rate constraints in the uplink of a multicarrier heterogeneous network. The major challenge in this formulation is represented by the minimum-rate requirements that cast the problem into a non-cooperative game in the sense of Debreu in which the actions sets of the players are coupled (and not independent as in the more popular Nash games). We used fractional programming techniques to characterize the game's equilibrium states (when they exist) as the fixed points of a water-filling operator. To attain this equilibrium in a distributed fashion, we also proposed an adaptive, distributed algorithm based on an iterative water-filling best response process and we provided sufficient conditions for its convergence. The convergence and the performance of our method was further assessed by numerical simulations: performance results show that reducing the non-radiative power consumed by the user device electronics, offloading the macrocell traffic through small cells, and increasing the number of receive antennas, are particularly critical to improve the performance of mobile terminals in terms of *both energy efficiency and spectral efficiency*. Using a reasonable simulation setup, we showed that the proposed framework is able to achieve significantly high area spectral efficiencies (larger than 1,000 b/s/Hz/km²), peak and cell-edge spectral efficiencies (up to 6 b/s/Hz and around 0.5 b/s/Hz, respectively), and energy efficiencies (several Mb/J), while considering dense populations of users (around 1,000 users/km²), low power consumptions (at most some Watts), a limited number of antennas (at most 8 for the small-cell access points and 16 for the macrocell base station), and a simplified signal processing at the receiver (maximal ratio combining).

The system model adopted in this work is general enough to encompass a more general *multi-cellular* and *multi-tier* network, and the derived approach can be thus automatically adapted to such scenarios. Moreover, distinguishing features of the proposed distributed algorithm are its *scalability* and *flexibility*, thus making it suitable to exploit all the available degrees of freedom of the network and to be adapted to emerging 5G technologies [46], such as ultra-densification and massive MIMO.

Challenging open issues for further work include: *i*) assessing the feasibility of the problem given a particular network realization for the multicarrier case; *ii*) assessing (and possibly reducing) the algorithm's complexity as a function of the system parameters; and *iii*) evaluating the impact of different receiver architectures (such as multiuser, zero-forcing, and interference cancellation techniques) on the spectral and energy efficiency of the network.

APPENDIX A PROOF OF PROPOSITION 1

First, note that (10) can be expressed in the language of fractional programming as:

$$\mathbf{p}_k^* = \arg \max_{\mathbf{p}_k \in \mathcal{P}_k(\mathbf{p}_{-k})} \frac{\varphi(\mathbf{p}_k)}{\chi(\mathbf{p}_k)} \quad (30)$$

where $\mathcal{P}_k(\mathbf{p}_{-k})$ is defined as in (11), and

$$\varphi(\mathbf{p}_k) = \sum_{n=1}^N \ln(1 + \mu_{k,n} p_{k,n}) \quad (31)$$

$$\chi(\mathbf{p}_k) = p_{c,k} + \sum_{n=1}^N p_{k,n}. \quad (32)$$

Using [26, Sect. II.A] we can see that solving problem (30) is equivalent to finding the root of the following nonlinear function:

$$\Phi(\lambda_k) = \max_{\mathbf{p}_k \in \mathcal{P}_k(\mathbf{p}_{-k})} \varphi(\mathbf{p}_k) - \lambda_k \chi(\mathbf{p}_k) \quad (33)$$

where $\lambda_k \in \mathbb{R}$. To compute the solution of (30), let us first use (31)-(32), but without the constraint (10b), so that $\mathbf{p}_k \in \mathbb{R}_+^N$ (i.e., only nonnegative powers are considered). The stationarity condition, given by

$$\left. \frac{\partial \varphi(\mathbf{p}_k)}{\partial p_{k,n}} \right|_{p_{k,n}=p_{k,n}^*} - \lambda_k \left. \frac{\partial \chi(\mathbf{p}_k)}{\partial p_{k,n}} \right|_{p_{k,n}=p_{k,n}^*} = 0 \quad (34)$$

for all $n = 1, \dots, N$ using (31) and (32) becomes

$$\frac{\mu_{k,n}}{1 + \mu_{k,n} p_{k,n}^*} - \lambda_k = 0 \quad n = 1, \dots, N. \quad (35)$$

Hence, considering $p_{k,n}^* \geq 0$, the optimal power allocation becomes the waterfilling criterion (18), in which the water level λ_k^* is replaced by λ_k . By plugging (35) back into (33), we can finally compute the optimal power level λ_k :

$$-\ln \lambda_k + (\beta_k - 1) = \alpha_k \lambda_k \quad (36)$$

where the functions α_k and β_k are defined as in (21) and (22), respectively. To provide a better insight on (36), let us try to write it in a closed form. To this aim, let us define $\nu_k = -\ln \lambda_k + (\beta_k - 1)$ so that (36) can be rewritten as $\nu_k e^{\nu_k} = \alpha_k e^{\beta_k - 1}$. Using the Lambert function $W(\cdot)$ we can obtain the expression of λ_k as in (20).

When introducing back the constraint (10b), we are placing a lower bound on $\varphi(\mathbf{p}_k)$: $\varphi(\mathbf{p}_k) \geq \theta_k$. Following [26], this is equivalent to placing an upper bound $\bar{\lambda}_k$ on λ_k , that comes out of the inverse waterfilling criterion that minimizes $\chi(\mathbf{p}_k)$ given $\varphi(\mathbf{p}_k) = \theta_k$, and is equal to (23). Hence, the solution to (10) is given by (18), with λ_k^* computed as in (19).

APPENDIX B

PROOF OF PROPOSITION 2

The DE \mathbf{p}^* exists and is unique if the mapping, represented by the best response vector $\mathcal{B}(\mathbf{p}) = [\mathcal{B}_1(\mathbf{p}_{-1}), \dots, \mathcal{B}_K(\mathbf{p}_{-K})]$, where $\mathcal{B}_k(\mathbf{p}_{-k}) = \arg \max_{\mathbf{p}_k \in \mathcal{P}_k(\mathbf{p}_{-k})} u_k(\mathbf{p})$ is user k 's best response to an interference vector \mathbf{p}_{-k} , is a contraction, , i.e., there exists a parameter $\varepsilon \in [0, 1)$ such that, for some norm,

$$\|\mathcal{B}(\mathbf{p}_1) - \mathcal{B}(\mathbf{p}_2)\| \leq \varepsilon \|\mathbf{p}_1 - \mathbf{p}_2\| \quad \forall \mathbf{p}_1, \mathbf{p}_2 \in \mathcal{P}, \quad (37)$$

where $\mathcal{P} = \prod_{k=1}^K \mathcal{P}_k$. The n th component of user k 's best response is given by $\mathcal{B}_{k,n}(\mathbf{p}_{-k}^*) = [\mathcal{B}_k(\mathbf{p}_{-k}^*)]_n = p_{k,n}^*$ as in (18).

Using [31, Theorem 4], the DE \mathbf{p}^* is unique is, for any UE k ,

$$\left\| \frac{\partial \mathbf{I}_k}{\partial \mathbf{p}_{-k}} \right\| \cdot \sup_{\mathbf{I}_k \in \mathbb{R}^N} \left\| \frac{\partial \mathcal{B}_k(\mathbf{p}_{-k})}{\partial \mathbf{I}_k} \right\| < 1. \quad (38)$$

The first part of (38) is explicitly computed in [31, Eq. (19)], and it is equal to

$$\left\| \frac{\partial \mathbf{I}_k}{\partial \mathbf{p}_{-k}} \right\| = \sqrt{\sum_{j=1, j \neq k}^K \sum_{n=1}^N \omega_{kj,n}^2}. \quad (39)$$

To compute the second part of (38), let us start by writing down the matrix $\partial \mathcal{B}_k(\mathbf{p}_{-k}) / \partial \mathbf{I}_k$:

$$\frac{\partial \mathcal{B}_k(\mathbf{p}_{-k})}{\partial \mathbf{I}_k} = \begin{pmatrix} \frac{\partial p_{k,1}^*}{\partial I_{k,1}} & \cdots & \frac{\partial p_{k,N}^*}{\partial I_{k,1}} \\ \vdots & \ddots & \vdots \\ \frac{\partial p_{k,1}^*}{\partial I_{k,N}} & \cdots & \frac{\partial p_{k,N}^*}{\partial I_{k,N}} \end{pmatrix}. \quad (40)$$

Therefore, we have to compute the term

$$\left\| \frac{\partial \mathcal{B}_k(\mathbf{p}_{-k})}{\partial \mathbf{I}_k} \right\| = \sqrt{\sum_{\ell=1}^N \sum_{n=1}^N \left| \frac{\partial p_{k,n}^*}{\partial I_{k,\ell}} \right|^2}. \quad (41)$$

To do this, we start by rewriting (18) in a more convenient way:

$$p_{k,n}^* = (1/\lambda_k^* - 1/\mu_{k,n}) \mathbb{1}_{\{\mu_{k,n} > \lambda_k^*\}}. \quad (42)$$

After some derivation steps, we obtain the norm of its partial derivative w.r.t. $I_{k,\ell}$ as follows:

$$\left| \frac{\partial p_{k,n}^*}{\partial I_{k,\ell}} \right|^2 = \frac{\mathbb{1}_{\{\mu_{k,n} > \lambda_k^*\}}}{\omega_{kk,\ell}^2 (\varsigma_k^*)^2} \cdot [\xi_{k,\ell}^2 + ((\varsigma_k^*)^2 - 2\varsigma_k^* \xi_{k,\ell}) \cdot \mathbb{1}_{\{n=\ell\}}], \quad (43)$$

where, for convenience, we denote by $\varsigma_k^* = |\mathcal{S}_k^*|$ and

$$\xi_{k,\ell} = -\varsigma_k^* \cdot \mu_{k,\ell}^2 \cdot \frac{\partial (1/\lambda_k^*)}{\partial \mu_{k,\ell}}. \quad (44)$$

By summing these terms over $n \in \{1, \dots, N\}$ we further have

$$\sum_{n=1}^N \left| \frac{\partial p_{k,n}^*}{\partial I_{k,\ell}} \right|^2 = \frac{1}{\varsigma_k^* \omega_{kk,\ell}^2} \cdot (\xi_{k,\ell}^2 + \varsigma_k^* - 2\xi_{k,\ell}) \cdot \mathbb{1}_{\{\mu_{k,\ell} > \lambda_k^*\}}. \quad (45)$$

It follows then that

$$\left\| \frac{\partial \mathcal{B}_k(\mathbf{p}_{-k})}{\partial \mathbf{I}_k} \right\| = \sqrt{\frac{1}{\varsigma_k^*} \sum_{\ell \in \mathcal{S}_k^*} \frac{1}{\omega_{kk,\ell}^2} \cdot (\xi_{k,\ell}^2 + \varsigma_k^* - 2\xi_{k,\ell})}. \quad (46)$$

Now, to prove that the terms $\xi_{k,\ell}$ in (44) are equivalent to (26) in Proposition 2, the reader is referred to Appendix C for the sake of clarity.

As a final step in the proof, notice that the function to be optimized in (24) depends only on $\mu_{k,n}$ which is an invertible, bijective function of $I_{k,n} \geq 0$ (since it is a strictly decreasing function w.r.t. $I_{k,n}$). Therefore, we can take the supremum over $\mu_{k,n} \in (0, \omega_{kk,n}^2/\sigma^2], \forall n$ directly.

APPENDIX C

COMPUTATION OF $\xi_{k,n}$

In this section, we compute $\xi_{k,\ell}$ in two different cases depending on the relative order between λ_k and $\overline{\lambda}_k$.

A. Minimum-rate waterfilling

Let us start from the minimum-rate waterfilling criterion, in which UE k 's water level is computed using (19). In this case, if $\mu_{k,\ell} > \overline{\lambda}_k$, i.e., if $\ell \in \overline{\mathcal{S}}_k$,⁴

$$\frac{1}{\overline{\lambda}_k} = \left(\frac{2^{N\theta_k}}{\prod_{n \in \overline{\mathcal{S}}_k} \mu_{k,n}} \right)^{1/\overline{\varsigma}_k} = \left(\frac{2^{N\theta_k}}{\prod_{n \in \overline{\mathcal{S}}_k, n \neq \ell} \mu_{k,n}} \right)^{1/\overline{\varsigma}_k} \cdot (\mu_{k,\ell})^{-1/\overline{\varsigma}_k}, \quad (47)$$

where $\overline{\varsigma}_k = |\overline{\mathcal{S}}_k|$. From this, it can be verified that

$$\frac{\partial (1/\overline{\lambda}_k)}{\partial \mu_{k,\ell}} = -\frac{1}{\overline{\varsigma}_k \mu_{k,\ell}} \cdot \frac{1}{\overline{\lambda}_k}, \quad (48)$$

and thus, using (44), $\xi_{k,\ell} = \mu_{k,\ell}/\overline{\lambda}_k$, corresponding to the first branch of (26).

B. Energy-efficient waterfilling

Let us now focus on the energy-efficient waterfilling, in which each UE k 's water level is computed using (20). If $\mu_{k,\ell} > \lambda_k$,

$$\frac{\partial (1/\lambda_k)}{\partial \mu_{k,\ell}} = \frac{1}{\lambda_k} \cdot \frac{\partial}{\partial \mu_{k,\ell}} [W(\alpha_k e^{\beta_k-1}) - (\beta_k - 1)] \quad (49)$$

$$= \frac{1}{\lambda_k} \cdot \left[\frac{\partial}{\partial \mu_{k,\ell}} W(\alpha_k e^{\beta_k-1}) - \frac{\partial}{\partial \mu_{k,\ell}} \beta_k \right]. \quad (50)$$

On the one hand, using (21) and (22), we can compute the partial derivatives $\frac{\partial \alpha_k}{\partial \mu_{k,\ell}} = \frac{1}{\varsigma_k \mu_{k,\ell}^2}$ and $\frac{\partial \beta_k}{\partial \mu_{k,\ell}} = \frac{1}{\varsigma_k \mu_{k,\ell}}$, with $\varsigma_k = |\mathcal{S}_k|$. On the other hand, using the properties of Lambert functions we have that

$$\frac{\partial}{\partial \mu_{k,\ell}} W(\alpha_k e^{\beta_k-1}) = \frac{W(\alpha_k e^{\beta_k-1}) \cdot \frac{\partial}{\partial \mu_{k,\ell}} (\alpha_k e^{\beta_k-1})}{(\alpha_k e^{\beta_k-1}) [1 + W(\alpha_k e^{\beta_k-1})]}. \quad (51)$$

Combining all these derivatives, we finally obtain

$$\frac{\partial (1/\lambda_k)}{\partial \mu_{k,\ell}} = \frac{W(\alpha_k e^{\beta_k-1}) - \alpha_k \mu_{k,\ell}}{\varsigma_k \mu_{k,\ell}^2 \lambda_k \alpha_k [1 + W(\alpha_k e^{\beta_k-1})]}. \quad (52)$$

⁴Note that we are interested in computing $\xi_{k,\ell}$ only for $\ell \in \overline{\mathcal{S}}_k$, as in all other cases $\xi_{k,\ell} = 0$. We will do the same for the energy-efficient waterfilling criterion.

Noting that, by inverting (20), $W(\alpha_k e^{\beta_k - 1}) = \beta_k - 1 - \ln \lambda_k$, and using similar steps as those taken in [33, Proof of Prop. 2], (27) can be rewritten as $\nu_k = W(\alpha_k e^{\beta_k - 1}) = \alpha_k \lambda_k$. Using (44), $\xi_{k,\ell}$ corresponds to the second branch of (26).

REFERENCES

- [1] “The 1000x data challenge,” Qualcomm, Tech. Rep. [Online]. Available: <http://www.qualcomm.com/1000x>
- [2] G. Auer *et al.*, *D2.3: Energy efficiency analysis of the reference systems, areas of improvements and target breakdown*. INFSO-ICT-247733 EARTH, ver. 2.0, 2012. [Online]. Available: <http://www.ict-earth.eu/>
- [3] Green Touch Consortium, Tech. Rep. [Online]. Available: <http://www.greentouch.org>
- [4] J. Hoydis, M. Kobayashi, and M. Debbah, “Green small-cell networks,” *IEEE Veh. Technol. Mag.*, vol. 6, no. 1, pp. 37 – 43, 2011.
- [5] D. Fudenberg and J. Tirole, *Game Theory*. Cambridge, MA: MIT Press, 1991.
- [6] W. Yu, G. Ginis, and J. Cioffi, “Distributed multiuser power control for digital subscriber lines,” *IEEE J. Sel. Areas Commun.*, vol. 20, no. 5, pp. 1105 – 1115, 2002.
- [7] N. Yamashita and Z.-Q. Luo, “A nonlinear complementarity approach to multiuser power control for digital subscriber lines,” *Optim. Methods and Software*, vol. 19, pp. 633 – 652, 2004.
- [8] R. Cendrillon, J. Huang, M. Chiang, and M. Moonen, “Autonomous spectrum balancing for digital subscriber lines,” *IEEE Trans. Signal Process.*, vol. 55, no. 8, pp. 4241 – 4257, 2007.
- [9] F. Meshkati, H. V. Poor, and S. C. Schwartz, “An energy-efficient approach to power control and receiver design in wireless data networks,” *IEEE Trans. Commun.*, vol. 53, no. 11, p. 1885, November 2005.
- [10] F. Meshkati, M. Chiang, H. V. Poor, and S. C. Schwartz, “A game-theoretic approach to energy-efficient power control in multicarrier CDMA systems,” *IEEE J. Sel. Areas Commun.*, vol. 24, pp. 1115–1129, 2006.
- [11] F. Meshkati, A. J. Goldsmith, H. V. Poor, and S. C. Schwartz, “A game-theoretic approach to energy-efficient modulation in CDMA networks with delay QoS constraints,” *IEEE J. Sel. Areas Commun.*, vol. 25, no. 6, pp. 1069–1078, August 2007.
- [12] G. Scutari, D. Palomar, and S. Barbarossa, “Optimal linear precoding strategies for wideband noncooperative systems based on game theory part I: Nash equilibria,” *IEEE Trans. Signal Process.*, vol. 56, no. 3, pp. 1230 – 1249, March 2008.
- [13] ———, “Optimal linear precoding strategies for wideband non-cooperative systems based on game theory – Part II: Algorithms,” *IEEE Trans. Signal Process.*, vol. 56, no. 3, pp. 1250 – 1267, March 2008.
- [14] ———, “Competitive design of multiuser MIMO systems based on game theory: A unified view,” *IEEE J. Sel. Areas Commun.*, vol. 26, no. 7, pp. 1089 – 1103, 2008.
- [15] P. Mertikopoulos, E. V. Belmega, and A. L. Moustakas, “Matrix exponential learning: Distributed optimization in MIMO systems,” in *ISIT ’12: Proceedings of the 2012 IEEE International Symposium on Information Theory*, 2012, pp. 3028–3032.
- [16] P. Coucheney, B. Gaujal, and P. Mertikopoulos, “Distributed optimization in multi-user MIMO systems with imperfect and delayed information,” in *ISIT ’14: Proceedings of the 2014 IEEE International Symposium on Information Theory*, 2014.
- [17] Y. Shi, J. Wang, K. Letaief, and R. Mallik, “A game-theoretic approach for distributed power control in interference relay channels,” *IEEE Trans. Wireless Commun.*, vol. 8, no. 6, pp. 3151 – 3161, 2009.
- [18] S. Ren and M. van der Schaar, “Distributed power allocation in multi-user multi-channel cellular relay networks,” *IEEE Trans. Wireless Commun.*, vol. 9, no. 6, pp. 1952 – 1964, 2010.
- [19] D. T. Ngo, L. B. Le, T. Le-Ngoc, E. Hossain, and D. I. Kim, “Distributed interference management in two-tier CDMA femtocell networks,” *IEEE Trans. Wireless Commun.*, vol. 11, no. 3, pp. 979 – 989, 2012.
- [20] G. Scutari, D. Palomar, F. Facchinei, and J.-S. Pang, “Convex optimization, game theory, and variational inequality theory,” *IEEE Signal Process. Mag.*, vol. 27, no. 3, pp. 35 – 49, 2010.
- [21] J.-S. Pang, G. Scutari, D. Palomar, and F. Facchinei, “Design of cognitive radio systems under temperature-interference constraints: A variational inequality approach,” *IEEE Trans. Signal Process.*, vol. 58, no. 6, pp. 3251 – 3271, 2010.
- [22] E. V. Belmega and S. Lasaulce, “Energy-efficient precoding for multiple-antenna terminals,” *IEEE Trans. Signal Processing*, vol. 59, no. 1, pp. 329–340, 2011.

- [23] E. V. Belmega, S. Lasaulce, and M. Debbah, "A survey on energy-efficient communications," in *Proc. IEEE Intl. Symp. Personal, Indoor and Mobile Radio Communications Workshops (PIMRC)*, Istanbul, Turkey, Sep. 2010, pp. 289–294.
- [24] E. Björnson, L. Sanguinetti, J. Hoydis, and M. Debbah, "Designing multi-user MIMO for energy efficiency: When is massive MIMO the answer?" in *Proc. IEEE Wireless Commun. and Networking Conf. (WCNC)*, Istanbul, Turkey, Apr. 2014.
- [25] G. Bacci, E. V. Belmega, and L. Sanguinetti, "Distributed energy-efficient power optimization in cellular relay networks with minimum rate constraints," in *Proc. IEEE Intl. Conf. Acoustics, Speech and Signal Process. (ICASSP)*, Florence, Italy, May 2014.
- [26] C. Isheden, Z. Chong, E. Jorswieck, and G. Fettweis, "Framework for link-level energy efficiency optimization with informed transmitter," *IEEE Trans. Wireless Commun.*, vol. 11, no. 8, pp. 2946–2957, Aug. 2012.
- [27] J. Nash, "Non-cooperative games," *Annals of Mathematics*, vol. 54, no. 2, pp. 286–295, 1951.
- [28] G. Debreu, "A social equilibrium existence theorem," *Proc. Natl. Acad. Sci. USA*, vol. 38, no. 10, pp. 886–893, October 1952.
- [29] F. Facchinei and C. Kanzow, "Generalized Nash equilibrium problems," *Quarterly J. Operations Research*, vol. 5, no. 3, pp. 173–210, Sep. 2007.
- [30] S. Boyd and L. Vandenberghe, Eds., *Convex Optimization*. Cambridge, UK: Cambridge Univ. Press, 2004.
- [31] G. Miao, N. Himayat, G. Li, and S. Talwar, "Distributed interference-aware energy-efficient power optimization," *IEEE Trans. Wireless Commun.*, vol. 10, no. 4, pp. 1323–1333, Apr. 2011.
- [32] G. Bacci, E. V. Belmega, and L. Sanguinetti, "Distributed energy-efficient power and subcarrier allocation for OFDMA-based small cells," in *Proc. IEEE Intl. Conf. Commun. (ICC) Workshop on Small Cell and 5G Networks*, Sydney, Australia, Jun. 2014.
- [33] G. Bacci, E. V. Belmega, P. Mertikopoulos, and L. Sanguinetti, "Energy-aware competitive link adaptation in small-cell networks," in *Proc. IEEE Int. Work. Resource Allocation in Wireless Net. (WiOpt - RAWNET)*, Hammamet, Tunisia, May 2014.
- [34] R. Corless, G. Gonnet, D. Hare, D. Jeffrey, and D. Knuth, "On the Lambert W function," *Adv. Comp. Math.*, vol. 5, pp. 329–359, 1996.
- [35] G. Miao, N. Himayat, and G. Li, "Energy-efficient link adaptation in frequency-selective channels," *IEEE Trans. Commun.*, vol. 58, no. 2, pp. 545–554, Feb. 2010.
- [36] C. Y. Wong, R. S. Cheng, K. B. Letaief, and R. D. Murch, "Multiuser OFDM with adaptive subcarrier, bit, and power allocation," *IEEE J. Select. Areas Commun.*, vol. 17, no. 10, pp. 1747–1758, Oct. 1999.
- [37] H. Tabassum, Z. Dawy, and M. S. Alouini, "Sum rate maximization in the uplink of multi-cell OFDMA networks," in *Proc. Intl. Wireless Commun. and Mobile Computing Conf.*, Istanbul, Turkey, Jul. 2011.
- [38] M. Chiang, P. Hande, T. Lan, and C. W. Tan, "Power control in wireless cellular networks," *Foundations and Trends in Networking*, vol. 2, no. 4, pp. 381–533, 2007.
- [39] G. Bacci, E. V. Belmega, P. Mertikopoulos, and L. Sanguinetti, "Energy-aware competitive link adaptation in heterogeneous networks," Tech. Rep., Jul. 2014. [Online]. Available: <http://www.ipt.unipi.it/l.sanguinetti/hetnets.pdf>
- [40] G. Scutari, D. Palomar, and S. Barbarossa, "Optimal linear precoding strategies for wideband noncooperative systems based on game theory – Part I: Nash equilibria," *IEEE Trans. Signal Process.*, vol. 56, no. 3, pp. 1230–1249, Mar. 2008.
- [41] G. Bacci, L. Sanguinetti, M. Luise, and H. V. Poor, "Energy-efficient power control for contention-based synchronization in OFDMA systems with discrete powers and limited feedback," *EURASIP J. Wireless Commun. and Networking (JWCN)*, vol. 2013, no. 1, Jul. 2013.
- [42] W. Dinkelbach, "On nonlinear fractional programming," *Management Science*, vol. 13, no. 7, pp. 492–498, Mar. 1967.
- [43] A. Adhikary, J. Nam, J.-Y. Ahn, and G. Caire, "Joint spatial division and multiplexing – The large-scale array regime," *IEEE Trans. Information Theory*, vol. 59, no. 10, pp. 6441–6463, Oct. 2013.
- [44] G. Calcev, D. Chizhik, B. Göransson, S. Howard, H. Huang, A. Kogiantis, A. F. Molisch, A. L. Moustakas, D. Reed, and H. Xu, "A wideband spatial channel model for system-wide simulations," *IEEE Trans. Veh. Technol.*, vol. 56, no. 2, pp. 389–403, Mar. 2007.
- [45] 3GPP Technical Specification Group, "LTE: Requirements for further advancements for Evolved Universal Terrestrial Radio Access (E-UTRA) (LTE-Advanced)," *Tech. Rep. 3GPP TR 36.913 v10.0.0*, Apr. 2011.
- [46] J. G. Andrews, S. Buzzi, W. Choi, S. Hanly, A. Lozano, A. C. K. Soong, and J. C. Zhang, "What will 5G be?" *IEEE J. Sel. Areas Commun.*, vol. 32, no. 9, September 2014.
- [47] E. Björnson, L. Sanguinetti, J. Hoydis, and M. Debbah, "Optimal design of energy-efficient multi-user MIMO systems: Is massive MIMO the answer?" submitted to *IEEE Trans. Wireless Comm.*, April 2014. [Online]. Available: <http://arxiv.org/abs/1403.6150>
- [48] S. Verdú, "On channel capacity per unit cost," *IEEE Trans. Information Theory*, vol. 36, no. 5, pp. 1019–1030, Sep. 1990.